International Scholars Journals

African Journal of Physics ISSN 9821-5213 Vol. 8 (5), pp. 001-013, May, 2021. Available online at www.internationalscholarsjournals.org © International Scholars Journals

Full Length Research Paper

Non-fitted prediction of Clay Soil aggregate shrinkage

V.Y. Chertkov

Faculty of Civil and Environmental Engineering, Technion, Haifa 32000, Israel. E-mail: agvictor@techunix.technion.ac.il

Accepted 08 September, 2020

All available models of soil shrinkage curves, despite their essential differences, are based on fitting the model parameters. We try to construct a model that enables one to predict the shrinkage curve based on physical parameters, that is, parameters that can be measured or calculated without fitting, independently of an experimental shrinkage curve. Such a model is constructed for real aggregates of clay soils (i.e., soils with clay content approximately > 40% by weight). The intra-aggregate matrix is considered to be a clay matrix that embraces silt and sand grains. An available microstructure- based model of the clay matrix shrinkage curve is used. For data analysis we derive an estimate for the liquid limit of the intra-aggregate matrix. We compare predicted and observed shrinkage curves using available data on aggregates of 31 different swelling soils that are mostly clay soils. As expected the generalized model works for clay soil aggregates with clay content approximately >40% (21 of 31 soils under study). The obtained results of the clay soil aggregates are a prerequisite of the next step relating to the shrinkage modeling of an aggregated soil without fitting.

Keywords: Modeling without fitting; shrinkage; aggregates; clay microstructure.

INTRODUCTION

A theoretical description and eventual prediction of the shrinkage curve of a swelling soil is of great interest because dependable modeling of the shrinkage characteristics of soils is an important prerequisite for the prediction of their hydraulic properties. For the present there are a number of approaches for obtaining the expressions describing observable shrinkage curves. A thermodynamics-based approach to clay-water systems enables the derivation of a shrinkage curve equation of a disaggregated clay soil at water contents below the air-entry point (Sposito, 1973; Sposito and Giraldez, 1976; Giraldez et al., 1983). A group of approaches are based on the different geometrization of experimental shrinkage curves as a combination of three straight lines (McGarry and Malafant, 1987), three straight lines (including basic or normal shrinkage (Mitchell, 1992)) and three curvilinear parts that are approximated by exponential equations (Braudeau et al., 2004) or polynomial equations (Tariq and Durnford, 1993) . Still another group of approaches is based on the approximation of experimental shrinkage curves by different parametric expressions (Nelder, 1961, 1962 - logistic model; Groenevelt and Bolt, 1972; Kim et al., 1992; Olsen and Haugen, 1998, Peng and Horn, 2005; Cornelis et al., 2006). With all their differences the above approaches have two important general features in common. First, all these approaches are based on either thermodynamic, i.e., macroscopic, considerations or experimental shrinkage curves. For this reason the approaches do not use concepts of both intra- and interaggregate soil structure in constructing the expression approximating a shrinkage curve. Second, the parameters of the approaches are only found by fitting of the model shrinkage curve to an experimental one. Even those parameters that are not formal and have a physical meaning cannot be measured independently of a shrinkage curve or calculated from such measurements.

A model that does not possess the two above limiting features has been recently proposed (Chertkov, 2000, 2003). The model relates to the shrinkage curve of a pure clay matrix or clay paste at different water contents. The model links the shrinkage curve of a clay matrix with its microstructure and pore-size distribution. Parameters of the model shrinkage curve can be found independently of the latter. The model was validated using relevant available data (Tessier and Pédro, 1984; Bruand and Prost, 1987). In this paper that model is referred to as the basic one. Lately, the basic model has been applied to the development of a physically based model for the water retention of clay pastes (Chertkov, 2004). One can consider the basic model as a semi-finished product or first step. The natural second step in developing the model is the transition to shrinkage of real aggregates because in any case the intra-aggregate matrix is a clay

matrix that, in general, embraces silt-sand grains and possible microcracks. The next step (beyond the scope of this work) is the transition to an aggregated soil. The objectives of this work are:

- to generalize the basic model to the case of paste-like mixture of clay, silt, and sand at sufficiently high clay content (approximately >40% by weight) and without cracks, i.e., to the case of an intra-aggregate clay soil matrix;
- to substantiate, using the basic model, a simple relation between the liquid limit of a clay soil and the moisture content of the clay soil aggregates at zero suction;
- to compare the shrinkage data from Bronswijk and Evers-Vermeer (1990) for aggregates of 31 different (mostly clay) swelling soils from the Netherlands and the results of the shrinkage curve prediction of the soil aggergates, based on the above generalization (see the first objective) and substantiation (see the second objective).

A detailed summary of the basic model, including the links between the shrinkage curve of a clay matrix and its microstructure, can be found in Chertkov (2003, 2004). Here, for the reader's convenience we start from a brief summary of the model points that are most necessary.

Brief summary of the basic model

Shrinkage curve of a clay matrix in relative coordinates

In the form $v(\zeta)$ where ζ is the relative water content of the clay, i.e., the ratio of the current value of the gravimetric water content to the maximum possible value - the liquid limit, and *v* is the relative volume of drying clay, the shrinkage curve of a clay matrix is presented as (Figure1).

$$v(\zeta) = \begin{cases} v_Z, & 0 \le \zeta \le \zeta_Z \\ v_Z + \dfrac{(1-v_S)^2}{4(v_Z - v_S)(1-F_Z)}(\zeta - \zeta_Z)^2, & \zeta_Z < \zeta \le \zeta_n \\ v_S + (1-v_S)\zeta, & \zeta_n < \zeta \le 1 \end{cases} \quad (1)$$

where v_Z and v_S are indicated in Figure 1;

$$\zeta_Z = \frac{v_Z - v_S}{1 - v_S} F_Z \quad (2)$$

is the shrinkage limit of the clay matrix; F_Z is the pore volume fraction occupied by water (saturation degree) at a water content corresponding to the shrinkage limit (ζ_Z); and

$$\zeta_n = \frac{(v_Z - v_S)(2 - F_Z)}{1 - v_S} \quad (3)$$

is the minimum water content in the normal shrinkage area (air-entry point).

Estimating the F_Z parameter

One can estimate F_Z from v_Z and v_S values, and then ζ_Z (Eq.(2)) and ζ_n (Eq.(3)) parameters of the pure clay, and thereby express the shrinkage curve of $v(\zeta)$ (Eq.(1)) through parameters v_S and v_Z only. In general, $0.11 \cong< v_Z < 1$ and $0.03 \cong< v_S < \min(v_Z \text{ and } \cong 0.2)$. In the case $v_Z = 0.11$ we have $F_Z = 0$ (and ζ_Z, ζ_n from Eqs.(2) and (3)). If $0.11 < v_Z < 1$

$$F_Z = \frac{f((X + \Delta X)/Y) - f(X/Y)}{1 - f(X/Y)} \quad (4)$$

where

$$f(x) = 1 - \exp(-\ln(6)(4x)^4 \exp(-4x)), \quad (5)$$

$$X \equiv \gamma v_Z - 1, \quad (6)$$

$$Y \equiv A\frac{v_Z}{v_S} - 1, \quad (7)$$

$$\Delta X \equiv (A\frac{v_Z}{v_S} - \gamma)v_Z, \quad (8)$$

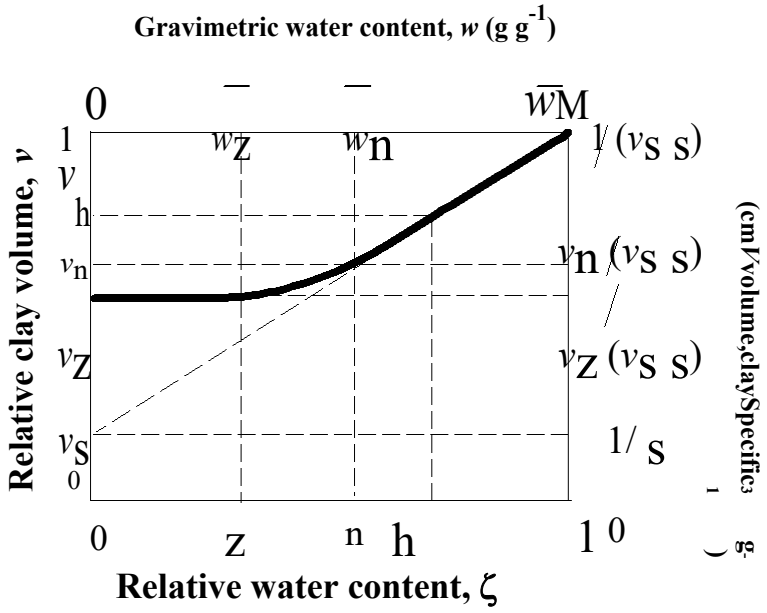

Figure 1. The general form of the shrinkage curve of a clay matrix (Chertkov's (2000). Fig.2) $\zeta = \zeta_h$ is the zero suction point.

and the constant values of $\gamma \cong 9$ and $A \cong 13.57$ flow out of the clay microstructure consideration.

Shrinkage curve of a clay matrix in customary coordinates

One can recalculate the dependence $v(\zeta)$ as the shrinkage curve of the clay matrix in the form $V(w)$ (the specific volume vs. gravimetric water content of the clay matrix; see Figure 1) using the $V \leftrightarrow v$ correspondency as

$$V = v/(v_S \rho_S), \quad (9)$$

and the $w \leftrightarrow \zeta$ correspondency as

$$w = \frac{(1 - v_S)\rho_W}{\rho_S}\zeta \quad (10)$$

where ρ_W is the density of water; and ρ_S is the density of the solid phase (clay particles). Similarly, one can recalculate the dependence $v(\zeta)$ as the shrinkage curve of the clay matrix in the form $e(\vartheta)$ (void ratio vs. moisture ratio of the clay matrix) using the $e \leftrightarrow v$ correspondency as

$$e = v/v_S - 1, \quad (11)$$

and the $\vartheta \leftrightarrow \zeta$ correspondency as

$$\vartheta = \frac{(1 - v_S)}{v_S}\zeta \quad (12)$$

Determination of the parameters of the clay matrix shrinkage curve

The ρ_S, v_S, and v_Z parameters can be found irrespective of the shrinkage curve of a clay matrix. The density of clay particles, ρ_S is measured by standard methods (Blake and Hartge, 1986). For a clay the minimum relative volume v_Z and the relative volume v_S of clay particles at the liquid limit, can be calculated from measured values of the specific volume of the clay matrix in oven-dried state, V_Z and the liquid limit, w_M of the clay matrix using Eqs.(9) and (10) at $v = v_Z$ and $\zeta = 1$, respectively. It is worth noting that, as applied to the shrinkage curve of a clay matrix, the immediately measured ρ_S, v_S, and v_Z parameters reflect the specifics of different physical-chemical processes that are connected with clay mineralogy, concentration and type of cations in water.

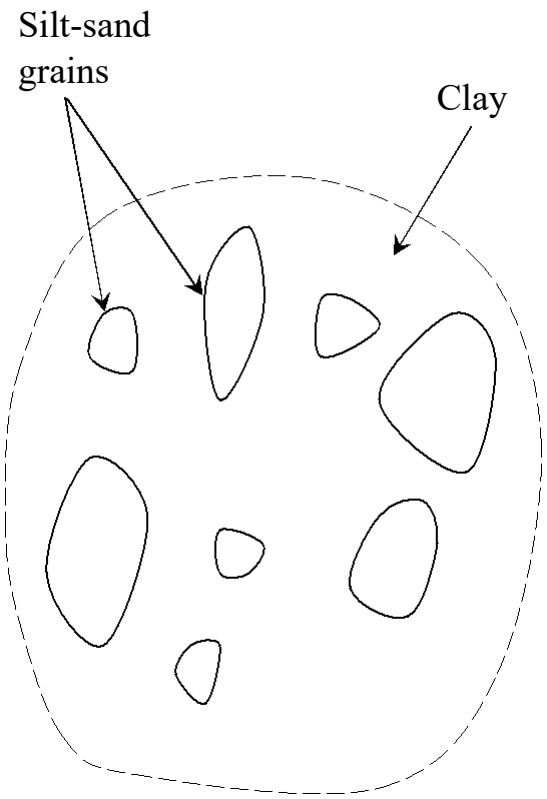

Figure 2. The assumed intra-aggregate matrix of a clay soil with sufficiently high clay content.

Some microstructure relations of a clay matrix

Connected or nearly connected clay particles outline micropores (matric pores). The dimension of connected clay particles increases and their thickness decreases with water content. The basic model gives the following estimates that will be needed below:

$$\Delta_Z \cong 0.03 r_{mZ} \quad (13)$$ and

$$\Delta_M \cong 0.01 r_{mM} \quad (14)$$

where Δ_Z is the thickness of plate-like clay particles of a clay matrix in the zero shrinkage area; Δ_M is that at the liquid limit; r_{mZ} is the maximum external dimension of pores (or the maximum dimension of clay particles) in the zero shrinkage area; and r_{mM} is that at the liquid limit (the external pore dimension includes the pore dimension itself and half thicknesses of two opposite clay particles from those outlining the pore).

Generalization of the basic model to the case of an intra-aggregate clay soil matrix

Our aim in this section is to generalize the basic model and to consider the shrinkage curve model of an intra-aggregate matrix that consists of a clay matrix embracing silt and sand grains and includes no cracks (Figure 2). Hereafter, the term “intra-aggregate matrix” only means such a structure as in Figure 2. We assume that this model can be applied to the intra-aggregate matrix of a clay soil with sufficiently high clay content (approximately >40% by weight). This assumption will be checked below using available data.

Relations between an intra-aggregate matrix and that of a corresponding pure clay

One can use the relative coordinates ξ and u for the swelling soil of any structure. ξ is the ratio of a current value of the gravimetric water content of the soil to the maximum possible value in the solid state (the liquid limit). u is the ratio of a current value of the soil volume to the maximum possible value of the volume. In the range $0 < \xi \le 1$ there are values ξ_Z and ξ_n of the shrinkage limit and air-entry point, respectively. Relative volumes u_Z and u_n correspond to the relative water contents ξ_Z and ξ_n. Finally, one can introduce a relative volume of the solid phase, u_S (the ratio of the volume of all solid components of the soil to the maximum possible volume of the latter), and a relative volume of the non-clay solid phase, u_S (the similar ratio for all solid components except for the the clay particles).

We are interested in the particular case of the swelling soil structure shown in Figure 2 - the intra-aggregate matrix. Only in this case are there simple linear relations between the water content (ξ) and volume (u) of the structure and those (ζ, v) of the corresponding pure clay matrix as

$$\zeta = \xi \quad (15)$$

and

$$v = (u - u_S)/(1 - u_S) . \quad (16)$$

These relations follow immediately from Figure 2 (coincidence of pore space of the intra-aggregate matrix and corresponding clay matrix) and the above definitions

of (ζ, v), (ξ, u), and u_S . In particular, it follows from Eq.(15) and the definitions of ζ_Z , ζ_n . ξ_Z , and ξ_n that

$$\zeta_Z = \xi_Z , \quad \zeta_n = \xi_n \cdot \qquad (17)$$

Similarly, it follows from Eq.(16) and the definitions of v_Z , v_S , u_Z , u_S , and u_S that

$$v_Z = (u_Z - u_S) /(1- u_S) \qquad (18)$$

and

$$v_S = (u_S - u_S) /(1- u_S) . \qquad (19)$$

The shrinkage curve of an intra-aggregate matrix in relative coordinates

According to Eqs.(15) and (17) in the presentation of the shrinkage curve of an intra-aggregate matrix one can use the same water content variable, ζ and water content parameters, ζ_Z and ζ_n that were used for the corresponding pure clay. Then the shrinkage curve of the intra-aggregate matrix (Figure 2) in relative coordinates, $u(\zeta)$ is obtained after replacement of v, v_Z , and v_S in Eq.(1) of the basic-model dependence, $v(\zeta)$ for the pure-clay matrix, from Eqs.(16), (18), and (19). The simple term rearrangement shows that the relative volume of the non-clay solid phase, u_S falls out of the $u(\zeta)$ dependence and the latter takes exactly the same form as Eq.(1) after replacement of all v values by u values

$$u(\zeta) = \begin{cases} u_z, & 0 \le \zeta \le \zeta_z \\ u_z + \dfrac{(1-u_s)^2}{4(u_z - u_s)(1-F_z)}(\zeta - \zeta_z)^2, & \zeta_z < \zeta \le \zeta_n \\ u_s + (1-u_s)\zeta, & \zeta_n < \zeta \le 1 \end{cases} \qquad (20)$$

The F_Z parameter in Eq.(20) keeps the same meaning and value as in Eq.(1). In the force of Eqs.(18) and (19) $(v_Z - v_S) /(1 - v_S) = (u_Z - u_S) /(1 - u_S)$. Therefore Eqs.(2) and (3) also keep the same form after the replacement of $v \to u$ as

$$\zeta_z = \frac{u_Z - u_S}{1 - u_S} F_z , \qquad (21)$$

$$\zeta_n = \frac{(u_Z - u_S)(2 - F_z)}{1 - u_S} . \qquad (22)$$

It is worth reiterating that ζ, ζ_Z , ζ_n and F_Z in Eqs.(1)-(3) and Eqs.(20)-(22) are the same, but $u \neq v$, $u_S \neq v_S$, $u_Z \neq v_Z$, and $u_n \neq v_n$ (see Eqs.(16), (18), and (19)). Thus, the $u(\zeta)$ curve of the intraaggregate matrix (Figure 2) is qualitatively similar to $v(\zeta)$ of clay matrix in Figure 1 with the replacement of v, v_Z , v_S , and v_n by u, u_Z , u_S , and u_n , respectively.

The shrinkage curve of an intra-aggregate matrix in customary coordinates

Relations that are given by Eqs.(9)-(12) are a particular case of similar relations for any soil. Therefore, one can recalculate the $u(\zeta)$ dependence as the shrinkage curve of the intra-aggregate matrix in the form, $U(w)$ (the specific volume vs. the gravimetric water content of the intra-aggregate matrix) using

$$U = u /(u_S \rho_S) \qquad (23)$$

and

$$w = \frac{(1- u_S)}{u_S} \frac{\rho_W}{\rho_S} \zeta \qquad (24)$$

where ρ_S is the average density of the solid phase. The $U(w)$ dependence of the intra-aggregate matrix is qualitatively similar to $\overline{V}(w)$ of the corresponding clay matrix in Figure 1. Similarly, one can recalculate the $u(\zeta)$ dependence as the shrinkage curve of the intra-aggregate matrix in the form $e(\vartheta)$ (the void ratio vs. the moisture ratio of the intra-aggregate matrix) using

$$e = u / u_S - 1 \qquad (25)$$

and

$$\vartheta = \frac{(1-u_S)}{u_S}\zeta . \qquad (26)$$

Estimating the F_Z parameter for the intra-aggregate matrix

The F_Z parameter entering Eq.(20) (and simultaneously Eq.(1)) can be estimated using u_Z , u_S , and u_S . First, using Eqs.(18) and (19) one finds the v_Z and v_S parameters of the corresponding clay matrix. Then the algorithm of subsection 2.2 permits one to estimate F_Z . The relative volume of the non-clay solid phase in the intra-aggregate matrix, u_S can be estimated preliminarily by the clay content and densities of different solid components (see section 6 and Appendix).

Determination of the parameters of the intra-aggregate-matrix shrinkage curve

Thus, in general, the shrinkage curve of an intra-aggregate matrix is determined by four parameters: ρ_S , u_Z , u_S , and clay content. All these parameters can be found irrespective of the shrinkage curve of the intra-aggregate matrix. ρ_S is measured by standard methods (Blake and Hartge, 1986). Clay content is also measured by standard methods (Gee and Bouder, 1986). Finally, u_Z and u_S can be calculated (similar to v_Z and v_S) from measured values of the specific volume of the intra-aggregate matrix in the oven-dried state, U_Z and the liquid limit, w_M of the intra-aggregate matrix, using Eqs.(23) and (24) at $u = u_Z$ and $\zeta = 1$, respectively.

A relation between the zero-suction point and the liquid limit

As one can see from the stated above, the liquid limit is an important parameter that is independent on the shrinkage curve, and at the same time determines one of its parameters (v_S or u_S). Our aim here is to suggest an estimated relation between the liquid limit and water content of a clay matrix at zero suction based on clay microstructure concepts from the basic model. This simple relation will be used in the following.

The zero suction point on the water content axis, ζ_h is between the air-entry point (Figure1, $\zeta = \zeta_n$) and the liquid limit ($\zeta = \zeta_M = 1$). This point corresponds to the maximum swelling of a clay matrix. Therefore, one can assume that at the zero-suction point, ζ_h the sizes of pore majority and clay particle majority outlining the pores are maximally possible for keeping the connections between the clay particles in their network, i.e., for keeping the network integrity. At a water content in the range $\zeta_h < \zeta < 1$ at least a part of the connections is broken. We assume that at ζ close to unity the separate disconnected clay particles make up the majority of all of them. Below we estimate the ζ_h value assuming the beginning of the network destruction at $\zeta > \zeta_h$, the majority of separate disconnected clay particles at ζ close to unity, and using the basic-model concepts. Figure 3a shows the two-dimensional illustrative scheme of a clay particle network before disconnections, i.e., at $\zeta \le \zeta_h$; r is a pore size. At a given ζ the r size varies between the minimum and maximum values. The maximum, $r_m(\zeta)$ depends on ζ. The maximum size of the separate clay particles after disconnections at $\zeta > \zeta_h$ is $r_{mh} = r_m(\zeta = \zeta_h)$. At a given ζ after disconnections (Figure 3b) the distance δr between clay particle edges varies between the minimum and maximum values. The maximum at a given ζ, $\delta r_m(\zeta)$ as a function of ζ reaches the maximum $\delta r_{mM} = \delta r_m(\zeta = 1)$ at $\zeta = \zeta_M = 1$. Thus, the volume of the clay particle system increases between water contents $\zeta = \zeta_h$ and $\zeta = \zeta_M = 1$ by $((r_{mh} + \delta r_{mM}) / r_{mh})^3$ times. That is (Figure 1),

$$v_M / v_h = 1/v_h = (1 + \delta r_{mM} / r_{mh})^3 . \qquad (27)$$

Let us estimate δr_{mM} . One can represent the maximum distance, δr_{mM} between clay particle edges at $\zeta = 1$ as

$$\delta r_{mM} = K \cdot \Delta_h \qquad (28)$$

where Δ_h is the mean thickness of disconnected clay particles, $\Delta(\zeta)$ at $\zeta > \zeta_h$. The clay particles are considered to be totally disconnected at the liquid limit,

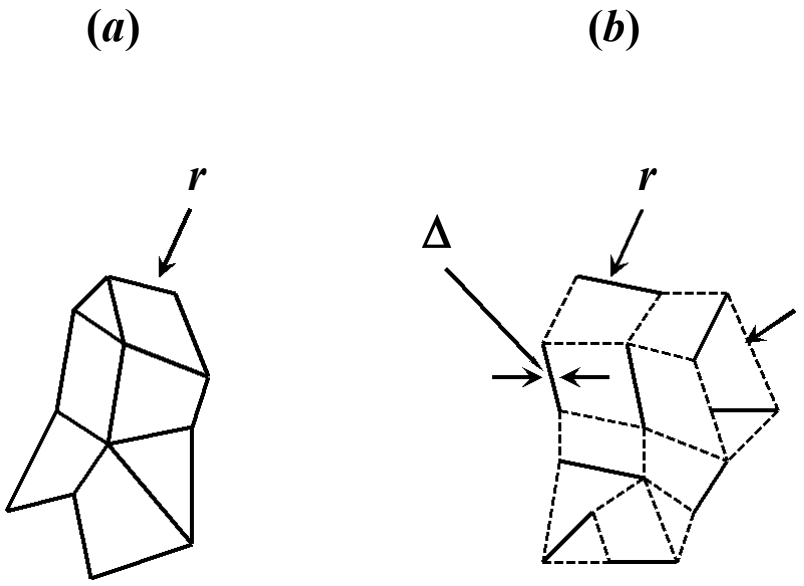

Figure 3. The two dimensional illustrative scheme of a clay particle network (a) before disconnections at $\zeta \leq \zeta_h$ and (b) after disconnections at $\zeta \cong \zeta_M = 1$. *r* is a clay particle (or pore) size; δr is a distance between the edges of the disconnected clay particles; Δ is the mean thickness of the clay particles.

$\zeta = \zeta_M = 1$ if $\delta r_{mM} >> \Delta_h$ (see Figure 3b), i.e., *K*>>1. Usually "much greater" sign means more than, at least by 10 times, i.e., $K \cong 10$. Replacing δr_{mM} in Eq.(27) from Eq.(28) at $K \cong 10$ one obtains

$$1/v_h \cong (1+10\Delta_h / r_{mh})^3. \quad (29)$$

Because $\zeta_z < \zeta_h < \zeta_M = 1$ (Figure 1) one can write the inequality.

$$\Delta_M / r_{mM} < \Delta_h / r_{mh} < \Delta_z / r_{mz}. \quad (30)$$

Accounting for Eqs.(13) and (14) and Eq.(30) one can rewrite Eq.(29) as $1.1^3 < 1/v_h < 1.3^3$. As an estimate we take $1/v_h = (1.1^3 + 1.3^3)/2 \cong 1.76$ and $v_h \cong 0.57$.

According to Eq.(1) one can write $v_h = v_s + (1 - v_s)\zeta_h$. Thus, ζ_h depends on v_s as $\zeta_h = (0.57 - v_s)/(1 - v_s)$. In the usual range $0.03 < v_s <\cong 0.2$ it gives $0.46 <\cong \zeta_h <\cong 0.55$. Accounting for that the above-accepted value of $K \cong 10$ is approximate, the variation of the ζ_h value within the limits of this range is not significant, and in the following it is reasonable to take the estimate of $\zeta_h \cong 0.5$.

Therefore, in the case of a clay matrix the ratio, $1/\zeta_h$ of the liquid limit to the water content corresponding to the zero suction value is approximately equal to two. In the case of an intra-aggregate matrix (Figure 2) the ratio of the liquid limit to the zero- suction water content is the same because pore spaces of the intra- aggregate matrix (Figure 2) and corresponding clay matrix coincide.

The feasibility of the above generalization of the basic model and the simple relation between the liquid limit and zero-suction water content (this section) will be checked in the following using available data.

Data used in this work for the model validation

We used data from Bronswijk and Evers-Vermeer (1990). The data were obtained on natural aggregates of seven soils in the Netherlands. Four-five horizons in the range of 0-110 cm were studied for each of the soil locations. The clay minerals of the seven profiles consist mainly of illite (30-40%) and smectite (20-40%). Table 1 reproduces the data from Bronswijk and Evers-Vermeer's

Table 1. Data that were used as input in checking the generalized model for aggregates of 31 soils from Bronswijk and Evers-Vermeer (1990): the density of clay particles, silt, and sand (ρ_s); the clay content (C_w) - the weight fraction of clay particles of mineral parts (clay, silt, and sand); $CaCO_3$ content (k_w) - the weight fraction of the soil; the organic matter content (o_w) - the weight fraction of the soil; the void ratio in the oven-dried state (e_z); and the void ratio at the zero-suction point (e_h)

Soil *no*.	Location	Depth (cm)	Horizon	ρ_s (g/cm^3)	C_w	k_w	o_w	e_z	e_h
1	Oosterend	0-22	A11	2.52	0.399	0	0.103	0.46	1.77
2		22-42	ACg	2.60	0.407	0	0.069	0.36	1.45
3		42-78	C1g	2.66	0.581	0.025	0.045	0.42	1.5
4		78-120	C2g	2.68	0.241	0.069	0.022	0.53	0.9
5	Nieuw Beerta	0-26	Ap	2.64	0.454	0.014	0.048	0.49	1.38
6		26-34	A12	2.61	0.459	0.008	0.039	0.47	1.5
7		34-56	C11g	2.62	0.516	0.017	0.022	0.48	1.66
8		56-75	C12g	2.68	0.391	0.033	0.019	0.50	1.40
9		75-107	C13g	2.69	0.593	0.003	0.030	0.56	1.63
10	Nieuw Statenzijl	0-29	Ap	2.65	0.520	0.090	0.033	0.45	1.32
11		29-40	AC	2.67	0.629	0.106	0.029	0.49	1.4
12		40-63	C21	2.69	0.524	0.113	0.027	0.56	1.68
13		63-80	C22g	2.66	0.558	0.098	0.028	0.57	1.65
14		80-100	C23g	2.69	0.596	0.116	0.022	0.58	1.8
15	Schermerhorn	0-21	A11	2.59	0.348	0.117	0.059	0.54	1.19
16		21-52	A12	2.61	0.429	0.111	0.062	0.54	1.58
17		52-77	C21g	2.62	0.321	0.176	0.037	0.82	1.60
18		77-100	C22g	2.63	0.162	0.188	0.031	0.80	1.10
19	Dronten	0-22	Ap1	2.66	0.368	0.099	0.026	0.47	1.07
20		22-38	A12	2.66	0.456	0.081	0.022	0.57	1.54
21		38-60	C22g	2.63	0.353	0.066	0.076	0.67	1.77
22		60-90	C23g	2.59	0.159	0.058	0.070	1.02	2.35
23		90-110	C24g	2.57	0.202	0.046	0.105	1.12	2.05
24	Bruchem	0-18	A11	2.52	0.581	0	0.099	0.29	1.5
25		18-30	A12	2.60	0.558	0	0.075	0.34	1.35
26		30-58	C11g	2.64	0.596	0	0.037	0.33	1.38
27		58-85	C12g	2.59	0.517	0	0.038	0.41	1.45
28	Kats	0-35	Ap	2.67	0.308	0.102	0.021	0.47	0.95
29		35-60	C21g	2.67	0.464	0.136	0.016	0.45	1.2
30		60-80	C22g	2.70	0.419	0.157	0.013	0.50	1.35
31		80-95	C23g	2.69	0.162	0.095	0.003	0.60	1.4

(1990) Table 1 on density of the solid phase (ρ_S), clay content (C_W), $CaCO_3$ content (k_W), and organic matter content (o_W). Figure 4 for soil *no.* 7 (Table 1) is representative for 21 soils with clay content $C_W >\cong 0.4$ (Table 1; soils *no*. 1-3, 5-14, 16, 20, 24-27, 29, 30). Figure 5 for soil *no.* 4 (Table 1) is representative for ten soils with clay content $C_W < 0.4$ (Table 1; soils *no*. 4, 15, 17-19, 21-23, 28, 31). Figures 4 and 5 reproduce the measured shrinkage curves in the form of $e(\vartheta)$ from Bronswijk and Evers-Vermeer (1990). These curves are shown by white circles. The black circle and triangle correspond to Bronswijk and Evers-Vermeer's (1990) data on air-entry point ($e_n = \vartheta_n$) and zero-suction point ($e_h = \vartheta_h$), respectively. In six cases the air-entry point and zero-suction point coincide (Table 1; soils *no*.3, 5, 8, 11, 27, and 28) The experimental void ratio in the oven-dried state, e_Z and the experimental e_h value for all the soils are given in Table 1. In addition to the input data that are presented in Table 1 we will need the density of

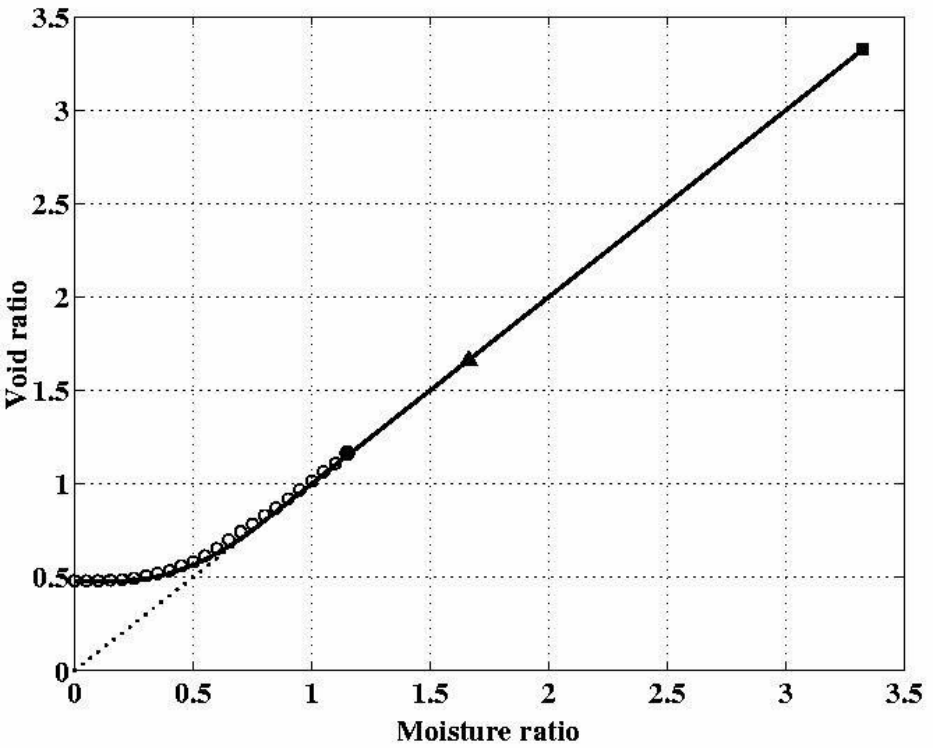

Figure 4. The shrinkage curve of natural aggregates of clay soil *no.* 7 (Table 1) from the Netherlands. White circles show the experimental curve (Bronswijk and Evers-Vermeer, 1990) . The black circle and triangle show the experimental air-entry point and zero-suction point, respectively. The solid line shows the model predicted curve. The black square shows the model predicted liquid-limit point.

solids of organic matter, ρ_O. We take below $\rho_O = 1.3 g \cdot cm^{-3}$ (Hillel, 1998, p.315, Table 12.1). Finally, it is worth reiterating that all input data from Table 1 and ρ_O were obtained independently of the measured shrinkage curves. Bronswijk and Evers-Vermeer (1990) note a broad variety of the soils under study, including those with relatively low clay content, and a strong variation of the shrinkage curves from one soil to another.

The maximum deflections of the separate experimental points of the averaged shrinkage curves plotted by Bronswijk and Evers- Vermeer (1990) in their original figures for soils *no.* 5, 6, 8, 9, 20, 31 (according to our numbering in Table 1) permit one to estimate the experimental standard deviation as $\delta e \cong 0.04$.

DATA ANALYSIS USING THE MODEL

Fitting of model parameters is widespread in soil science as a way of demonstrating a correspondence between data and a model. Therefore, it is worth emphasizing that the following checking of the generalized model and the ratio of the liquid limit to the zero- suction water content is based on the way that is usual in physics and consists of two steps. The former is the model prediction of a shrinkage curve for a given set of input data. The latter is the comparison between the predicted and the observed shrinkage curves. They are considered to be in compliance if discrepancies between them are within the limits of the experimental standard deviations, δe .

Unfortunately, Bronswijk and Evers-Vermeeer (1990) do not give data on the liquid limit of the soils under study. For this reason we cannot separately check that the ratio of the liquid limit to zero-suction water content is approximately equal to two, and then the generalized model. Therefore, the model and the approximate ratio value will be checked together.

Predicting a shrinkage curve for a given set of ρ_S , C_W , k_W , o_W , e_Z and e_h from Table 1 and the above ρ_O value, we consider two variants. In the former variant we take into account the presence of $CaCO_3$ and organic matter. With that we assume that the solid density of clay particles, silt, sand, and $CaCO_3$ coincide.

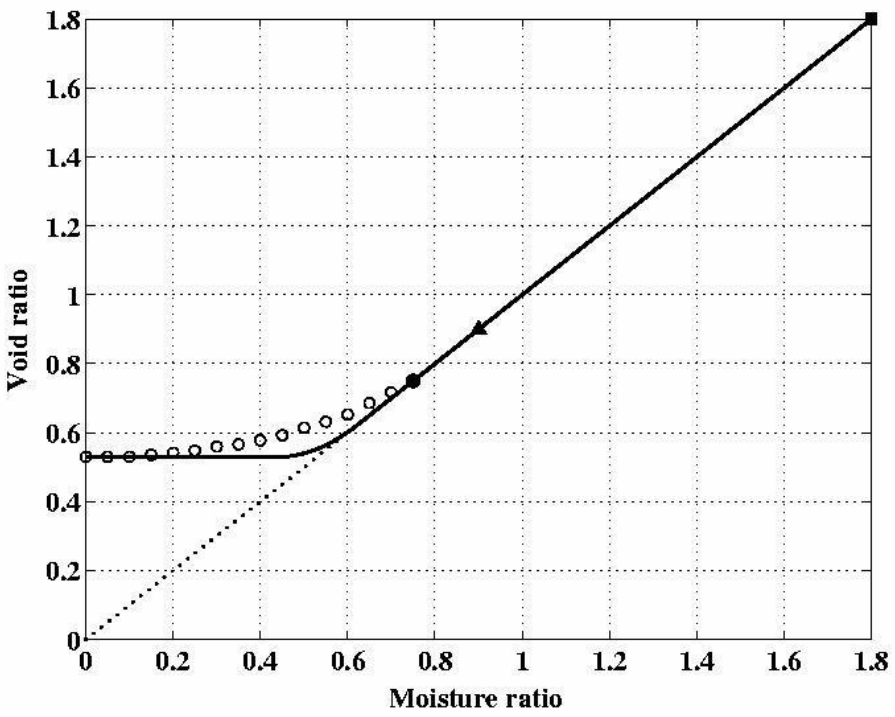

Figure 5. As in figure 4 for soil no.4 (Table 1).

Furthermore, in this variant we neglect any small possible change of $CaCO_3$ and organic matter content with drying. In the latter variant we neglect the presence of $CaCO_3$ and organic matter. Results of these two variants will be compared in the next section. The scheme of the shrinkage curve prediction in the first variant for a given set of ρ_S, C_W, k_W, o_W, ρ_O, e_Z and e_h is as follows.

1. Knowing e_h one can estimate the void ratio at the liquid limit, e_M as

$$e_M \cong 2e_h . \quad (31)$$

2. From Eq.(25) at $\zeta = 0$ ($e = e_Z$, $u = u_Z$) and at $\zeta = 1$ ($e = e_M$, $u = 1$), one estimates u_S and u_Z as

$$u_S = 1/(e_M + 1) , \; u_Z = (e_Z + 1)/(e_M + 1) . \quad (32)$$

From ρ_S, ρ_O, o_W, k_W, and C_W one estimates (see Appendix)

3. $$c_V = C_W (1 - k_W - o_W)/[1 + (\rho_S/\rho_O - 1) \cdot o_W] \quad (33)$$

where c_V is the volume fraction of clay solids of the total solids.

4. Because $1 - c_V$ is the volume fraction of non-clay solids of the total solids one estimates.

$$u_S = (1 - c_V) \cdot u_S . \quad (34)$$

5. Then one estimates v_Z and v_S from Eqs.(18) and (19).

6. Based on v_Z and v_S one estimates F_Z from Eqs.(4)-(8).

7. Based on u_S, u_Z, and F_Z one estimates ζ_Z and ζ_n from Eqs.(21) and (22), and after that the shrinkage curve in the form $u(\zeta)$ from Eq.(20).

8. Finally, using the $u(\zeta)$ curve and Eqs.(25)-(26) one can predict the shrinkage curve in the form $e(\vartheta)$.

9. Additionally, one can successively estimate (see Appendix)

$$o_V = \rho_S \cdot o_W / [\rho_S \cdot o_W + \rho_O (1 - o_W)] , \quad (35)$$

where o_V is the volume fraction of organic-matter solids of the total solids, the average density of solids, $\overline{\rho}_S$ as

$$\overline{\rho}_S = \rho_S (1 - o_V) + \rho_O o_V , \quad (36)$$

and the liquid limit in terms of gravimetric water content (from Eq.(24) at $\zeta = 1$, $w = w_M$ and Eq.(25) at $u = 1$, $e = e_M$) as

$$w_M = e_M \cdot \rho_W / \overline{\rho}_S . \quad (37)$$

In the second variant when we neglect the presence of $CaCO_3$ and organic matter, the ρ_O, k_W, and o_W data are not needed; c_V (Eq.(33)) that is used in Eq.(34) coincides with C_W; and in additional point 9 ~~$\rho_S = \rho_S$~~ and $w_M = e_M \cdot \rho_W / \rho_S$.

RESULTS AND DISCUSSION

Figure 4 for soil *no.* 7 (Table 1) is typical for 21 soils with clay content $C_W >\cong 0.4$ (Table 1; soils *no*. 1-3, 5-14, 16, 20, 24-27, 29, 30). Figure 5 for soil *no.* 4 (Table 1) is typical for ten soils with clay content $C_W < 0.4$ (Table 1; soils *no*. 4, 15, 17-19, 21-23, 28, 31). Figures 4 and 5 show the model predicted $e(\vartheta)$ curves (solid lines) and (ϑ_M, e_M) points (black squares) for the variant accounting for the presence of $CaCO_3$ and organic matter. Calculations according to the second variant, when we neglect the presence of $CaCO_3$ and organic matter, showed that model predicted shrinkage curves that were obtained with and without accounting for the presence of $CaCO_3$ and organic matter, practically coincide.

The comparison between the experimental and the corresponding model predicted shrinkage curves for aggregates of 21 soils with clay content, $C_W >\cong 0.4$ by weight (see Figure 4 as an example), visually shows the agreement between them within the limits of the experimental standard deviations, $\delta e \cong 0.04$ for 20 soils and a small discrepancy only in the case of soil *no.* 13. This discrepancy is likely connected to random reasons, e.g., with a little larger experimental error than for other soils. In connection with soil *no*.13 it should be noted that the use in future direct data on the liquid limit (e_M or w_M) will enable one to raise the prediction accuracy of the shrinkage curve. Except for that the direct e_M data permit a specification of the estimated relation between e_M and e_h (Eq.(31)) accounting for a slight dependence of the relation on v_S. Thus, the major result is as follows: for all the soils under study with clay content $>\cong 40\%$ by weight, the discrepancies between experimental and predicted shrinkage curves of soil aggregates are within the limits of the experimental standard deviation, $\delta e \cong 0.04$.

The comparison between the experimental and the corresponding model predicted shrinkage curves for aggregates of ten soils with clay content, $C_W < 0.4$ by weight (see Figure 5 as an example), visually shows that discrepancies between them are out of the limits of the experimental standard deviations. This is expected. With that, the largest discrepancies take place for the five soils with especially small C_W (Table 1, see soil *no*.4 - $C_W = 0.241$, soil *no*.18 - $C_W = 0.162$, soil no.22 - $C_W = 0.159$, soil *no*.23 - $C_W = 0.202$, and soil *no*.28 - $C_W = 0.308$). Appreciable, but weaker discrepancies take place for four soils with a little larger $C_W \cong 0.32 - 0.37$ (soils *no*.15, 17, 19, and 21). Finally, the unexpectedly small discrepancy between the data and prediction for soil *no*.31 with small $C_W = 0.162$ is likely due to random reasons. In any case the ratio value, $v_Z / v_S = 5.13$, that was found in the course of calculations for this soil *no.* 31, is out of the limits of a physical range ($v_Z / v_S \leq 3$) for pure clays (Chertkov, 2000). This fact shows that the unexpectedly small discrepancy between the generalized model and data for this soil is formal and random.

These comparison results lead to two major consequences:

- the generalized model and ratio, $e_M / e_h \cong 2$ work at the sufficiently high clay content of soil aggregates, at least, > 40% by weight (i.e., for clay soils);
- at the sufficiently low clay content (< 40% by weight) the generalized model is not applicable (that was expected).

Four approximations were accepted:

- we neglected the possible intra-aggregate microcracks in the structure frame of Figure 2 at the basic-model

generalization;

- we neglected the possible dependence of ζ_h on v_S in estimating the ratio of the liquid limit to the zero-suction water content.
- we neglected the possible differences between solid densities of clay, silt, and sand at the shrinkage curve prediction for Bronswijk and Evers-Vermeer's (1990) data; and

- we neglected the presence of $CaCO_3$ and organic matter in the second variant of the shrinkage curve prediction for Bronswijk and Evers-Vermeer's (1990) data.

The above mentioned results and their consequences show that at sufficiently high clay content (>40% by weight) all the four approximations are reasonable because their effects are within the limits of experimental errors. In particular, the volume of intra-aggregate microcracks is negligible at high clay content. A similar result was obtained in the basic model as applied to data from Bruand and Prost (1987) on a clay-silt-sand mixture of high clay content. Finally, inapplicability of the model under study at a low clay content is natural and expected. In this case the intra-aggregate structure, unlike that in Figure 2, is assumably a combination of a silt-sand skeleton with small aggregates in the pores of the latter. The volume of such an intra-aggregate structure should include an essential contribution of the microcrack-like voids.

Summary and Conclusion

An earlier proposed model permits one to predict the shrinkage curve of a clay matrix without fitted parameters and to link the shrinkage curve to the clay matrix microstructure and pore size distribution. The input data include the minimum relative volume of a clay matrix (v_Z), the relative volume of clay particles at the maximum water content (v_S), and the density of the clay particles (ρ_S). These parameters have a clear physical meaning and can be measured or calculated without fitting, independently of the experimental shrinkage curve. This work considers the natural second step in developing the model, the transition to shinkage of real aggregates, because in any case the intra-aggregate matrix at sufficiently high clay content is a clay matrix that, in general, embraces silt-sand grains and possible microcracks. We consider relations between the intra-aggregate matrix and the matrix of a corresponding pure clay. The relations enable a generalization of the shrinkage curve expression of a clay matrix to the shrinkage curve expression of an intra-aggregate matrix in the relative and customary coordinates (i.e., the specific volume vs. the gravimetric water content or the void ratio vs. the moisture ratio). Four physical parameters determine the shrinkage curve of clay soil aggregates: the minimum relative volume of the intra-aggregate matrix (u_Z), the relative volume of the solid phase of the intra-aggregate matrix at maximum water content (i.e., at the liquid limit) (u_S), the average density of the solid phase (ρ_S), and the weight fraction of the clay of the soil mineral components (clay, silt, and sand) (C_W).

These parameters can be measured irrespective of the shrinkage curve, i.e., without fitting. Then we derive a clay microstructure-based relation between the water content corresponding to the zero-suction point of clay soil aggregates and the liquid limit of the latter. This relation is then used in the data analysis. For the model validation we use the shrinkage data from Bronswijk and Evers-Vermeer (1990) for aggregates of 31 different swelling soils (mostly clay soils, i.e., with clay content > 40% by weight) from the Netherlands. The comparison between the experimental and model predicted shrinkage curves of 21 data sets with sufficiently high clay content (approximately > 40% by weight) shows that the differences between them are within the limits of experimental error. For the other ten data sets, however, the differences are out of the limits of experimental error. That is, as expected, the generalized model works at a sufficiently high clay content of clay soil aggregates, at least, > 40% by weight. The obtained results, relative to modeling the shrinkage of clay soil aggregates, are a prerequisite of the next step (beyond the scope of this work), that is the transition to shrinkage modeling of an aggregated soil without fitted parameters.

Acknowledgement

The research was supported in part by the Technion Water Research Institute.

Appendix

The volume fraction of organic-matter solids of the total solids, o_V is found as follows. According to definitions of ρ_O , ρ_S , o_V , and o_W one can write

$$o_W = \rho_O \cdot o_V / [\rho_O \cdot o_V + \rho_S (1 - o_V)] . \qquad \text{(A1)}$$

Solving Eq.(A1) one obtains the o_V value that was indicated in Eq.(35) and permits one to estimate o_V from the data of Table 1 and ρ_O .

The volume fraction, c_V of clay solids of the total solids, is found as follows. From definitions of k_W , o_W , and C_W (Table 1) one can write the weight fraction of clay of the soil, c_W as

$$c_W = C_W (1 - k_W - o_W) . \quad \text{(A2)}$$

The ratios, $c_V /(1 - o_V)$ and $c_W /(1 - o_W)$ give the volume and weight fractions of clay solids of the summary clay, silt, sand, and $CaCO_3$ solids. Because ρ_S is considered to be similar for clay, silt, sand, and $CaCO_3$, these ratios coincide. That is,

$$c_V = c_W \cdot (1 - o_V) /(1 - o_W) . \quad \text{(A3)}$$

Replacing in Eq.(A3) c_W from Eq.(A2) and o_V from Eq.(35) we obtain the c_V value that was indicated in Eq.(33) which permits us to estimate c_V from Table 1 and ρ_O .

REFERENCES

Blake GR, Hartge KH (1986). Particle density. In: A. Klute (ed.) Methods of soil analysis. Part 1. 2nd ed. Agron. Monogr. 9. ASA and SSSA, Madison, WI. pp.377-382.

Braudeau E, Sene M, Mohtar RH (2004) Characterizing nonrigid aggregated soil-water medium using its shrinkage curve. Soil Sci. Soc. Am. J. 68: 359-370.

Bronswijk JJB, Evers-Vermeer JJ (1990). Shrinkage of Dutch clay soil aggregates. Neth. J. Agric. Sci. 38: 175-194.

Bruand A, Prost R (1987) Effect of water content on the fabric of a soil material: an experimental approach. J. Soil Sci. 38: 461-472.

Chertkov VY (2000). Modeling the pore structure and shrinkage curve of soil clay matrix. Geoderma 95: 215-246.

Chertkov VY (2003). Modelling the shrinkage curve of soil clay pastes. Geoderma 112: 71-95.

Chertkov VY (2004). A physically based model for the water retention curve of clay pastes. J. Hydrol. 286: 203-226.

Cornelis WM, Corluy J, Medina H, Hartmann R, van Meirvenne M, Ruiz M.E. (2006) A simplified parametric model to describe the magnitude and geometry of soil shrinkage. Eur. J. Soil Sci. 57: 258-268.

Gee GW, Bauder JW (1986). Particle-size analysis. pp.383-411. *In*: A. Klute (ed.) Methods of soil analysis. Part 1. 2nd ed. Agron. Monogr. 9. ASA and SSSA, Madison, WI.

Giraldez JV, Sposito G, Delgado C (1983). A general soil volume change equation: I. The two-parameter model. Soil Sci. Soc. Am. J. 47, 419-422.

Groenevelt PH, Bolt GH (1972). Water retention in soil. Soil Sci. 113(4): 238-245.

Hillel D (1998). Environmental Soil Physics. Academic Press, New York.p. 771.

Kim DJ, Vereecken H, Feyen J, Boels D, Bronswijk JJB (1992). On the characterization of properties of an unripe marine clay soil. I. Shrinkage processes of an unripe marine clay soil in relation to physical ripening. Soil Sci. 153(6): 471-481.

McGarry D, Malafant KW (1987). The analysis of volume change in unconfined units of soil. Soil Sci. Soc. Am. J. 51, 290-297.

Mitchell AR (1992). Shrinkage terminology: Escape from “normalcy”. Soil Sci. Soc. Am. J. 56, 993-994.

Nelder JA (1961). The fitting of a generalization of the logistic curve. Biometrics 17, 89-110.

Nelder JA (1962). An alternative form of a generalized logistic equation. Biometrics 18, 614-616.

Olsen PA, Haugen LE (1998). A new model of the shrinkage characteristic applied to some Norwegian soils. Geoderma 83: 67-81.

Peng X, Horn R. (2005) Modeling soil shrinkage curve across a wide range of soil types. Soil Sci. Soc. Am. J. 69, 584-592.

Sposito G (1973). Volume changes in swelling clays. Soil Science 115(4), 315-320.

Sposito G, Giraldez JV (1976). Thermodynamic stability and the law of corresponding states in swelling soils. Soil Sci. Soc. Am. J. 40: 352-358.

Tariq AR, Durnford DS (1993). Analytical volume change model for swelling clay soils. Soil Sci. Soc. Am. J. 57: 1183-1187.

Tessier D, Pédro G (1984). Recherches sur le rôle des minéraux argileux dans l’organisation et le comportement des sols. In Livre Jubilaire du Cinquantenaire, AFES. pp. 223-234.